ELSEVIER

Carbohydrate Research 293 (1996) 147–172

CARBOHYDRATE RESEARCH

Structural characterisation of xyloglucan secreted by suspension-cultured cells of *Nicotiana plumbaginifolia*

Ian M. Sims [a], Sharon L.A. Munro [b], Graeme Currie [a], David Craik [c], Antony Bacic [a,*]

[a] *Cooperative Research Centre for Industrial Plant Biopolymers and Plant Cell Biology Research Centre, School of Botany, University of Melbourne, Parkville, Victoria 3052, Australia*

[b] *Victorian College of Pharmacy, Monash University, Parkville, Victoria 3052, Australia*

[c] *Centre for Drug Design and Development, University of Queensland, St. Lucia, Queensland 4072, Australia*

Received 6 February 1996; accepted in revised form 20 May 1996

Abstract

Linkage analysis of a xyloglucan from the extracellular medium of suspension cultures of *Nicotiana plumbaginifolia* showed mostly 4-Glc*p* and 4,6-Glc*p*, terminal Xyl*p* and 2-Xyl*p*, and terminal Ara*f*, along with ~ 10% (w/w) *O*-acetyl groups, equivalent to ~ 0.28 mol acetyl per mol of glycosyl residue. Methylation with methyl trifluoromethanesulfonate under neutral conditions, followed by re-methylation with CD_3I under basic conditions, and conversion into partially methylated alditol acetates showed that *O*-acetyl groups were primarily attached to C-6 of ~ 44% of the 4-Glc*p* backbone not substituted with Xyl*p* residues and to C-5 of ~ 15% of the terminal Ara*f* residues. These positions of the *O*-acetyl groups were confirmed by ^{1}H-NMR. Oligosaccharides generated by digestion of native xyloglucan with endo-(1 → 4)-β-glucanase were separated by a combination of gel-filtration chromatography and anion-exchange HPLC, and analysed by glycosyl linkage analysis and by electrospray ionisation–mass spectrometry (ESI–MS). The major oligosaccharide subunits were Glc_4Xyl_2 and Glc_5Xyl_2, of which 50–60% are substituted with one terminal Ara*f* residue attached to O-2 of a Xyl*p* residue, and a further 20–25% are substituted with two terminal Ara*f* residues attached to O-2 of the Xyl*p* residues. ESI–MS showed that many

Abbreviations: ESI–MS, electrospray ionisation–mass spectrometry; GLC–MS, gas chromatography–mass spectrometry; NMR, nuclear magnetic resonance; amu, atomic mass units; ppm, parts per million; D, daltons

* Corresponding author.

PII S0008-6215(96)00142-5

of the oligosaccharide subunits carried one, two and, occasionally three *O*-acetyl groups. © 1996 Elsevier Science Ltd.

Keywords: *Nicotiana plumbaginifolia*; Xyloglucan; *O*-Acetylation; Linkage analysis; Electrospray ionisation; Mass spectrometry; NMR

1. Introduction

Xyloglucans are structurally important polysaccharides in the cell walls of most dicotyledonous flowering plants and gymnosperms [1–4]. They consist of a backbone of (1 → 4)-β-D-Glc*p* residues which are branched at O-6 to α-D-Xyl*p* residues [1–3,5,6]. Digestion of many xyloglucans with endo-(1 → 4)-β-glucanase (EC 3.2.1.4), which cleaves unsubstituted (1 → 4)-β-D-Glc*p* residues, yields several oligosaccharides which have the basic heptasaccharide repeating unit XXXG (where each (1 → 4)-β-D-Glc*p* residue of the backbone is given a one-letter code according to its substituents [7]). Octa-, nona-, and undeca-saccharide units are derived from substitutions at O-2 of some of the α-D-Xyl*p* residues with β-D-Gal*p* residues or α-L-Fuc*p*-(1 → 2)-β-D-Gal*p* disaccharides [8].

Xyloglucan isolated from leaves of *Nicotiana tabacum* does not have the typical heptasaccharide repeating structure of most xyloglucans [9,10]. Less than half of the (1 → 4)-β-D-Glc*p* backbone residues on this xyloglucan are branched at O-6 to α-D-Xyl*p* residues, compared to 75% in most xyloglucans. From the results of digestion with endo-(1 → 4)-β-glucanase it was proposed that the major repeating unit of *N. tabacum* xyloglucan was XXG, with approximately half of the α-D-Xyl*p* residues substituted at O-2 with α-L-Ara*f* to give SXG/XSG [10]. However, the location of the remaining unsubstituted backbone residues was not determined. The xyloglucan from *N. tabacum* does not contain β-D-Gal*p* or α-L-Fuc*p*. Xyloglucans with a similarly low degree of branching have also been isolated from other Solanaceous plants: such a xyloglucan has been isolated from *Solanum tuberosum* [11], and recently, we have isolated such a xyloglucan from the extracellular polysaccharides (ECPs) of *N. plumbaginifolia* cell-suspension cultures [12].

The occurrence of *O*-acetyl groups on plant cell-wall polysaccharides is probably widespread, and has been reported for a number of different classes of polysaccharide [6], including xyloglucans from *Medicago sativus* (alfalfa) [13] and *Acer pseudoplatanus* (sycamore) cell-suspension cultures [14]. Detailed analysis of the major nonasaccharide repeating unit of xyloglucan from *A. pseudoplatanus* showed that *O*-acetyl groups were located predominantly on the β-D-Gal*p* residues. Analysis by proton nuclear magnetic resonance (^{1}H-NMR) showed that 55–60% of the *O*-acetyls were on C-6, 15–20% were on C-4 and 20–25% were on C-3, and that approximately 20% of the Gal*p* residues were not acetylated, 50% were monoacetylated, and 25–30% were diacetylated [15]. It has recently been reported that xyloglucans secreted by suspension-cultured *Nicotiana* (tobacco) and *Lycopersicon* (tomato) cells are *O*-acetylated at C-6 of the β-D-Glc*p* backbone, instead of on side-chain glycosyl residues [16]. *O*-Acetyl groups may be common substituents of many xyloglucans and other polysaccharides, but

they are not usually detected in molecules isolated from cell walls because of their lability in the strong alkaline conditions used for solubilisation [2].

In this paper, we report the structure of xyloglucan secreted by *N. plumbaginifolia* suspension cultures. High-performance liquid chromatography (HPLC) following NaOH treatment was used to determine the degree of *O*-acetylation of the xyloglucan. The precise location of *O*-acetyl groups on the backbone and side-chains of the xyloglucan was determined using sequential methylation, under neutral and then basic conditions, and by ^{1}H-NMR. The major oligosaccharides produced by digestion of xyloglucan with endo-(1 → 4)-β-glucanase were separated by a combination of gel-filtration chromatography and anion-exchange HPLC, and analysed by methylation analysis and by electrospray ionisation–mass spectrometry (ESI–MS).

2. Experimental

Purification of xyloglucan.—Xyloglucan was purified from ECPs of *N. plumbaginifolia* using a combination of anion-exchange chromatography and precipitation with saturated $(NH_4)_2SO_4$, as described previously [12] and is designated native xyloglucan. Deacetylated xyloglucan was prepared by dissolving native xyloglucan (10 mg) in 0.1 M NaOH (5 mL) and incubating for 2 h at room temperature and then dialysing against deionised water (molecular weight cut-off 6000) and freeze-drying. Xyloglucan from tamarind (*Tamarindus indicus*) seeds was from Megazyme, Australia.

Enzymic digestion of xyloglucan.—Native (5 mg) and deacetylated (5 mg) xyloglucan were separately dissolved in 20 mM NH_4OAc (20 mL, pH 4.0) and digested with α-L-arabinofuranosidase from *Aspergillus niger* (1.4 mg protein, 2 U, Megazyme) at 40 °C. Fractions (0.5 mL) were removed at intervals, the reaction stopped by heating for 10 min at 100 °C, and the product precipitated in 80% (v/v) EtOH. De-arabinosylation was monitored by linkage analysis of the ethanol-precipitated material (see later).

Native xyloglucan (200 mg) was dissolved in 20 mM NH_4OAc (20 mL, pH 4.5) and incubated with endo-(1 → 4)-β-glucanase from *Trichoderma viride* (2.7 mg protein, 20 U; Megazyme) at 40 °C. Fractions (2 mL) were removed at intervals and the reaction stopped by heating for 10 min at 100 °C. Undegraded material was removed by precipitation with 80% (v/v) EtOH, and the 80% EtOH-soluble oligosaccharides were concentrated under diminished pressure at 40 °C, and freeze-dried. Digestion of the xyloglucan was monitored by anion-exchange HPLC (see below). Deacetylated xyloglucan (5 mg, 1 mg mL^{-1} in 20 mM NH_4OAc) was digested with endo-(1 → 4)-β-glucanase (0.14 mg protein, 1 U) at 40 °C for 8 h and processed in the same way as digests of native xyloglucan.

Gel-filtration chromatography.—Xyloglucan oligosaccharides (20 mg) were dissolved in deionised water (1 mL) and separated on a column (190 × 2.2 cm i.d.) of Fractogel TSK HW-40(S) (Merck, Darmstadt, Germany) eluted with deionised water at 30 mL h^{-1}. Fractions (2 mL) were tested for carbohydrate (see below) and those corresponding to individual oligosaccharide size-classes were pooled, concentrated under diminished pressure at 40 °C, and freeze-dried. The column was calibrated with a series of (1 → 4)-β-D-oligoglucosides prepared by acid hydrolysis of cellulose (Sigma) in 2.5 M CF_3CO_2H for 10 min at 100 °C [17].

Anion-exchange chromatography.—Mixtures of total unfractionated xyloglucan oligosaccharides (100 μg) were dissolved in deionised water (1 μg μL^{-1}) and separated by anion-exchange HPLC at a flow rate of 1 mL min^{-1} on a Dionex BioLC using a CarboPac PA-1 column (4 × 250 mm; Dionex Corp., Sunnyvale, CA, USA) equilibrated in 150 mM NaOH. Oligosaccharides were eluted with a linear gradient of NaOAc (0–250 mM) in 150 mM NaOH over 40 min, starting 1 min after sample injection, and monitored using pulsed amperometric detection (Dionex). The column was calibrated with a series of (1 → 4)-β-D-oligoglucosides (see above).

Xyloglucan oligosaccharides (400 μg) of individual size-classes isolated by gel-filtration chromatography (see above) were separated on a Dionex CarboPac PA-1 preparative column (9 × 250 mm) at a flow rate of 5 mL min^{-1}. The major peaks (5 and 6) from the gel-filtration column (see Fig. 3) were injected in 150 mM NaOH containing 60 mM NaOAc, and eluted with a linear gradient of NaOAc (60–250 mM) in 150 mM NaOH over 40 min, starting 5 min after sample injection. Peak fractions were collected and neutralised with AcOH immediately after collection. Sodium ions were removed on a Dowex 50W-X8, H^+ column (Bio-Rad Laboratories) at 4 °C (to prevent cleavage of acid-labile terminal Ara*f* residues), and the purified oligosaccharides concentrated under diminished pressure at 40 °C.

Analytical methods.—Total carbohydrate was determined by the phenol-sulfuric method [18] using glucose (0–80 μg) as the standard.

Degree of acetylation.—The degree of acetylation was determined by saponification of native xyloglucan and measurement of released AcOH by HPLC [19]. Native xyloglucan (30 mg) was dissolved in a mixture of 2-propanol and 0.8 M NaOH (1:1), incubated at room temperature for 2 h, then centrifuged (10 000 g, 5 min). The acetic acid released was chromatographed at a flow rate of 0.6 mL min^{-1} on an Aminex HPX-87H column (7.8 × 300 mm, BioRad) eluted with 5 mM H_2SO_4, and detected by refractive index. Acetic acid was quantified by reference to a standard curve of glacial acetic acid (0–3 μg), and the degree of acetylation expressed as % w/w and as mol acetyl per mol glycosyl residues. (The average molecular weight of a glycosyl residue was calculated from the relative proportions of pentose and hexose in xyloglucan determined by linkage analysis.)

Electrospray–mass spectrometry (ESI–MS).—ESI–MS spectra were acquired using a Finnigan (Bremen, Germany) electrospray source attached to a Finnigan MAT 95 mass spectrometer, as described previously [20], and scanning from 300–3000 amu at 15 decade s^{-1}.

Linkage analysis.—Two different methylation procedures, under neutral [21] and basic [22] conditions, were employed to establish both the positions of the glycosidic linkages and the *O*-acetyl groups.

Methylation under basic conditions was performed using the NaOH method of [22]. Samples (20–100 μg) were dissolved in Me_2SO (50 μL) and methylated, extracted and dried as previously described [20], except that for oligosaccharide samples the first aliquot of CH_3I was added immediately after the addition of the NaOH slurry.

Methylation under neutral conditions was performed using the method of [21]. Carbohydrates (50–200 μg) were suspended in trimethyl phosphate (200 μL) by sonication. 2,6-Di-(*tert*-butyl)pyridine (50 μL) and methyl trifluoromethanesulfonate

(20 μL) were added, and samples incubated for 2 h at 50 °C. Reactions were stopped by addition of water (2 mL) and the methylated products extracted into $CHCl_3$ (1 mL) and dried. In certain cases the permethylated carbohydrates were then resuspended in Me_2SO and remethylated with CD_3I under basic conditions, as just described. In this way free hydroxyl groups were substituted with CH_3 groups and acetylated hydroxyl groups were then deacetylated and substituted with CD_3 groups.

Permethylated carbohydrates were hydrolysed with 2.5 M CF_3CO_2H (4 h, 100 °C), reduced with 1 M $NaBD_4$ overnight at room temperature and acetylated with Ac_2O (2 h, 100 °C). The resulting partially methylated alditol acetates were separated by GC on a fused-silica capillary column (25 m × 0.22 mm i.d.) with a high-polarity bonded phase BPX70 (SGE, Australia) and analysed by MS using a Finnigan MAT 1020B (San Jose, CA, USA) GLC–MS [23].

NMR spectroscopy.—Xyloglucan oligosaccharides (5 mg) were dissolved in 0.6 mL of deuterium oxide (D_2O, 99.99 atom %), with 3 μL of Me_2SO added as internal standard. Samples were then transferred to 5 mm NMR tubes (Wilmad Glass Co., 535-PP). Spectra were recorded on a Bruker AMX600 spectrometer, operating at a ^1H frequency of 600.13 MHz. All experiments were recorded at 27.3 °C. The probe temperature was controlled using a B-VT1000E unit and a Haake cooling bath, and had been calibrated using MeOH [24].

2D spectra were recorded in phase-sensitive mode using a time-proportional phase incrementation [25]. The 2D experiments used included a double quantum filtered scalar correlated spectroscopy (DQF-COSY) experiment [26] and two total correlation spectroscopy (TOCSY) [27,28] experiments using a DIPSI-2 Spin lock sequence [29]. Mixing times of 20 and 60 ms were used for the TOCSY experiments. The residual Me_2SO was irradiated via presaturation during the relaxation delay of all experiments.

The DQF-COSY spectrum was acquired with 768 t_1 increments, and both the TOCSY spectra were acquired with 512 t_1 increments. The ^1H spectral widths in all three spectra were 4201.7 Hz in both dimensions, over 4K complex data points in F_2. Data from the TOCSY spectra were zero-filled in F_1 to at least 1K data points, with the DQF-COSY spectrum also being zero-filled in F_2 to 4K data points. During processing, either a 90° or 60° phase-shifted sine bell or sine bell squared window was applied to the data in both dimensions. Polynomial baseline correlation was applied in selected regions of each spectrum and chemical shifts were referenced to internal Me_2SO as 2.71 ppm [30]. All processing was performed using standard Bruker software (UXNMR) on a Silicon Graphics 4D/30 personal Iris.

3. Results and discussion

Location of O*-acetyl groups.*—Quantitation of the degree of *O*-acetyl substitution by HPLC showed that the xyloglucan from *N. plumbaginifolia* ECPs contained ~ 10% (w/w) *O*-acetyl groups. This is equivalent to ~ 0.28 mol acetyl per mol of glycosyl residues (based on an average molecular weight of a glycosyl residue of 150 D, calculated from 36 mol% pentose (132 D) and 63 mol% hexose (162 D), Table 1).

In order to identify the sites of *O*-acetylation, native xyloglucan was methylated under both basic conditions, which release *O*-acetyl substituents, and neutral conditions,

Table 1
Linkage composition of native *Nicotiana plumbaginifolia* xyloglucan methylated under basic and neutral conditions. Neutral methylations were with methyl trifluoromethanesulfonate, and basic methylations were with either CH_3I or CD_3I

Sugar	Methyl substitution	Deduced structure and glycosidic linkage [a]	Linkage composition (mol%) [b]			
			Methylation conditions			
			Basic (CH_3I)	Neutral	Neutral then basic (CH_3I)	Neutral then basic (CD_3I)
Ara*f*	2,3,5-tri-*O*-CH_3	terminal	15	10	13	11
	2,3-di-*O*-CH_3,5-*O*-CD_3	terminal, with 5-*O*-Ac	– [c]	–	–	2
	2,3-di-*O*-CH_3	5-	–	3	–	–
Xyl*p*	2,3,4-tri-*O*-CH_3	terminal	10	14	15	15
	3,4-di-*O*-CH_3	2-	11	11	11	11
Gal*p*	2,3,4,6-tetra-*O*-CH_3	terminal	1	–	1	1
Glc*p*	2,3,4,6-tetra-*O*-CH_3	terminal	–	–	1	1
	2,3,6-tri-*O*-CH_3	4-	37	18	34	19
	2,3-di-*O*-CH_3-6-*O*-CD_3	4-, with 6-*O*-Ac	–	–	–	15
	2,3-di-*O*-CH_3	4,6	25	44	24	24

[a] Terminal Ara*f* is deduced from 1,4-di-*O*-acetyl-2,3,5-tri-*O*-methylarabinopentitol, etc.
[b] Average of duplicate determinations.
[c] –, Not detected.

which do not hydrolyse these alkali-labile substituents. Linkage analysis, using methylation under basic conditions, showed that xyloglucan from *N. plumbaginifolia* ECPs contained mostly 4-Glc*p* and 4,6-Glc*p*, terminal Xyl*p* and 2-Xyl*p*, and terminal Ara*f*, and small amounts of terminal Gal*p* (Table 1). When xyloglucan was methylated under neutral conditions with methyl trifluoromethanesulfonate and converted into partially methylated alditol acetates the proportion of 4-Glc*p* decreased by ~ 19 mol% with a corresponding increase in 4,6-Glc*p*, and the proportion of terminal Ara*f* decreased by ~ 4 mol%, coinciding with the appearance of an approximately equal amount of 5-Ara*f* (Table 1). These changes in linkage composition suggested that *O*-acetyl groups were present at O-6 of ~ 50% of the 4-Glc*p* residues and at O-5 of ~ 20% of the terminal Ara*f* residues.

Methylation of xyloglucan under neutral conditions followed by remethylation with CH_3I under basic conditions and conversion into partially methylated alditol acetates gave a linkage composition similar to that for xyloglucan methylated under basic conditions alone (Table 1). Neutral methylation followed by methylation under basic conditions with CD_3I enabled the location of the *O*-acetyl substituents to be confirmed, and the molar ratios of unsubstituted and substituted residues to be calculated more accurately. 4-Glc*p* and terminal Ara*f* were the only *O*-acetylated residues detected by these methylations (Table 1).

EI mass spectra of derivatives corresponding to 4-Glc*p* and terminal Ara*f* residues separated by GC are shown in Fig. 1. In addition to the diagnostic ions for the 4-Glc*p* derivative, a primary fragment ion at *m/z* 236 (and the respective secondary fragment ions) indicated that a CD_3 group was present at O-6 of a proportion of the derivatives

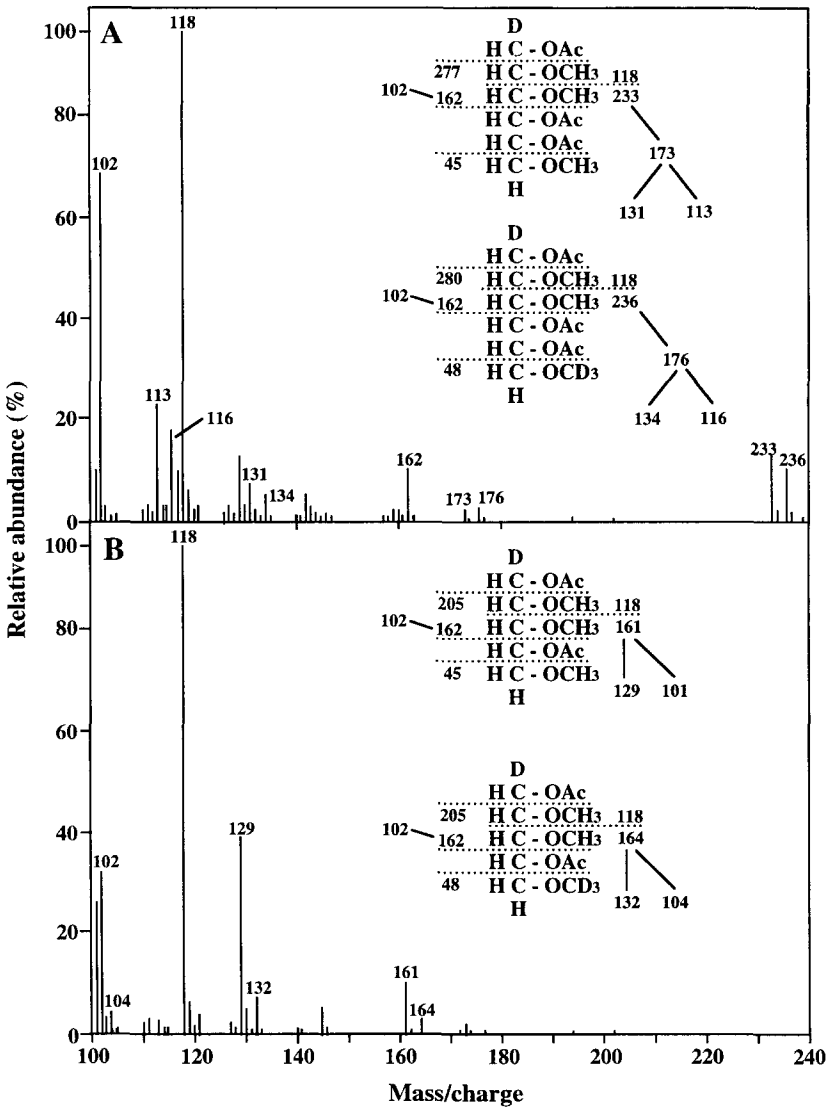

Fig. 1. EI–MS of material co-chromatographing with derivatives of 4-Glc*p* (A) and terminal Ara*f* (B) methylated under neutral conditions with methyl trifluoromethanesulfonate, followed by methylation under basic conditions with CD_3I. Fragmentation patterns are shown for a mixture 1,4,5-tri-*O*-acetyl-2,3,6-tri-*O*-methylhexitol and 1,4,5-tri-*O*-acetyl-2,3-di-*O*-methyl-6-*O*-trideuterio-methylhexitol (A), and for a mixture 1,4-di-*O*-acetyl-2,3,5-tri-*O*-methylpentitol and 1,4-di-*O*-acetyl-2,3-di-*O*-methyl-5-*O*-trideuterio-methylpentitol (B).

from this residue (Fig. 1A). Thus, the site of *O*-acetylation on 4-Glc*p* is at C-6. The EI mass spectrum of the terminal Ara*f* derivative contained ions diagnostic of this residue together with a primary fragment ion at *m/z* 164 (and the respective secondary fragment

ions), indicating that a CD_3 group was present at O-5 of a proportion of the derivatives from this residue (Fig. 1B). Thus, the site of *O*-acetylation on terminal Ara*f* is at C-5, although an ion at *m/z* 121 indicated that a small proportion (< 5%), from the ratio of *m/z* 118 (1,4-di-*O*-acetyl-2,3,5-tri-*O*-methylpentitol) to *m/z* 121 (1,4-di-*O*-acetyl-3,5-di-*O*-methyl-2-*O*-trideuteriomethylpentitol), of *O*-acetyls may also be present at C-2 of this residue.

From the ratio of ions having *m/z* 233 (1,4,5-tri-*O*-acetyl-2,3,6-tri-*O*-methylhexitol) to *m/z* 236 (1,4,5-tri-*O*-acetyl-2,3-di-*O*-methyl-6-*O*-trideuterio-methylhexitol) of derivatised native xyloglucan, compared to deacetylated controls, the degree of *O*-acetylation of the deduced 4-Glc*p* residue was calculated to be 44 mol%. Similarly, from the ratio of *m/z* 161 (1,4-di-*O*-acetyl-2,3,5-tri-*O*-methylpentitol) to *m/z* 164 (1,4-di-*O*-acetyl-2,3-di-*O*-methyl-5-*O*-trideuterio-methylpentitol) of derivatised native xyloglucan, compared to deacetylated controls, the degree of *O*-acetylation of the deduced terminal Ara*f* residue was calculated to be 15 mol%. The total degree of *O*-acetylation calculated from the degree of *O*-acetylation of 4-Glc*p* (37 mol% × 0.44) and terminal Ara*f* (15 mol% × 0.15) was ~ 0.19 mol acetyl per mol of glycosyl residues. This was lower than that determined by HPLC (0.28 mol acetyl per mol glycosyl residues) following deacetylation with NaOH, although it was equivalent to ~ 7% (w/w), and thus only slightly less than the 10% (w/w) determined by HPLC (see earlier).

Enzyme digestion of xyloglucan.—Digestion of native xyloglucan with α-L-arabinofuranosidase removed ~ 70 mol% of the terminal Ara*f* residues after 24 h digestion, but further incubation did not remove more Ara*f* residues (data not shown). Treatment of deacetylated xyloglucan with arabinofuranosidase removed over 95 mol% of the terminal Ara*f* residues after 24 h digestion. These data suggested that the α-L-arabinofuranosidase did not remove terminal Ara*f* residues which were *O*-acetylated.

Digestion of native *N. plumbaginifolia* xyloglucan with endo-(1 → 4)-β-glucanase was rapid compared with that of tamarind xyloglucan, and 98% (w/w) of the material was soluble in 80% ethanol after only 60 min incubation at 40 °C. In contrast, the enzyme-digested tamarind xyloglucan was less than 50% (w/w) ethanol-soluble after 60 min and after 24 h digestion was still only 87% (w/w) ethanol-soluble. Anion-exchange HPLC showed that the pattern of oligosaccharides obtained from *N. plumbaginifolia* xyloglucan did not change significantly after 4 h digestion up to 24 h digestion (data not shown). Anion-exchange HPLC of native xyloglucan digested for 8 h showed a complex pattern of oligosaccharides with two major peaks at retention times 28.2 min (N1) and 30.0 min (N2), respectively (Fig. 2A), and smaller amounts of glucose and cellobiose (identified by co-chromatography). Anion-exchange HPLC of deacetylated xyloglucan digested for 8 h showed a distinctly different pattern of oligosaccharides (Fig. 2B). This digest contained considerably more glucose and cellobiose than native xyloglucan digests, and contained three other major peaks at retention times 18.7 min (D1), 25.9 min (D2) and 26.8 min (D3). The N1 and N2 peaks, predominant in the digests of native xyloglucan (Fig. 2A), were virtually absent from the digests of deacetylated xyloglucan (Fig. 2B).

Linkage analysis under basic conditions of the total unfractionated endo-(1 → 4)-β-glucanase digests of native and deacetylated xyloglucan, soluble in 80% (v/v) ethanol, showed that oligosaccharides from deacetylated xyloglucan contained approximately

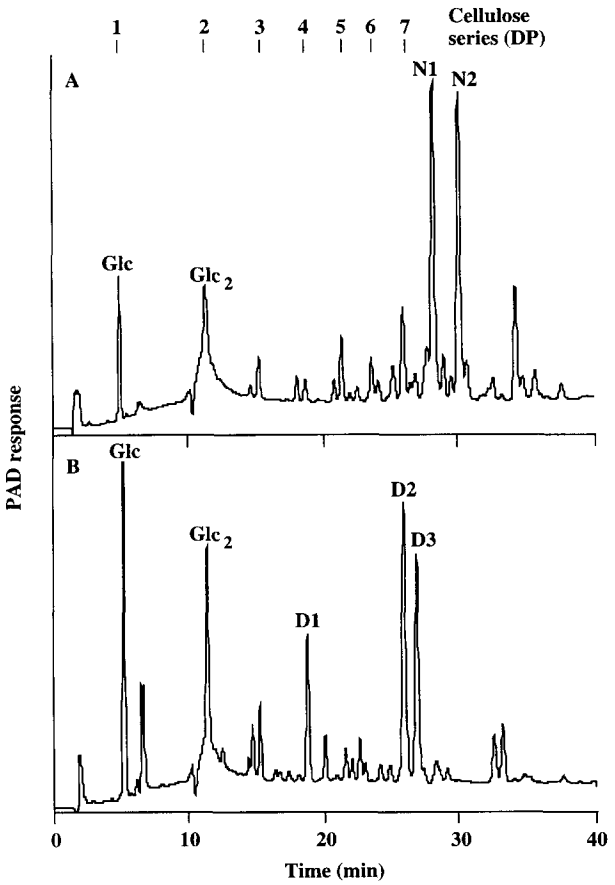

Fig. 2. Anion-exchange HPLC of native (A) and deacetylated (B) *Nicotiana plumbaginifolia* xyloglucan digested for 8 h with endo-(1 → 4)-β-glucanase. The oligosaccharides were separated on a CarboPac PA-1 column equilibrated in 150 mM NaOH and eluted with a linear gradient of NaOAc (0–250 mM) over 40 min, starting 1 min after sample injection. The eluted material was detected by pulsed amperometric detection. The column was calibrated with a series of (1 → 4)-β-D-oligoglucosides (degree of polymerisation 1–7); 1 and 2 show the elution positions of glucose (Glc) and cellobiose (Glc_2), respectively. Fractions N1 and N2 from the digests of native xyloglucan and D1, D2 and D3 from the digests of deacetylated xyloglucan were collected for linkage analysis.

half as much 4-Glc*p* (15 mol% versus 30 mol%) than oligosaccharides from native xyloglucan, with a corresponding increase in the amount of terminal Glc*p* (from 4 to 14 mol%) and 4,6-Glc*p* (from 13 to 18 mol%, Table 2). There was also a small decrease in the amount of 6-Glc*p* (from 11 to 8 mol%). The proportions of terminal Ara*f*, terminal Xyl*p* and 2-Xyl*p* were approximately equal in the two digests. The increase in terminal Glc*p* was consistent with the observed increase in glucose and cellobiose in deacetylated xyloglucan digests (Fig. 2). The changes in the relative proportions of 6-Glc*p* and 4,6-Glc*p* suggested that there were differences in the branched oligosaccharides in

Table 2
Linkage composition of native and deacetylated *Nicotiana plumbaginifolia* xyloglucan digested with endo-(1 → 4)-β-D-glucanase, and of individual oligosaccharide fractions from the digests obtained by anion-exchange HPLC (Fig. 2). Samples were methylated under basic conditions with CH_3I, converted to partially methylated alditol acetates, and analysed by GC–MS

Sugar	Deduced glycosidic linkage [a]	Linkage composition (mol%) [b]						
		Native xyloglucan			Deacetylated xyloglucan			
		Total digest	HPLC fraction		Total digest	HPLC fraction		
			N1	N2		D1	D2	D3
Ara*f*	terminal	17	13	11	15	– [c]	18	14
Xyl*p*	terminal	13	21	15	17	37	21	17
	2-	13	12	10	12	1	15	10
Gal*p*	terminal	–	–	–	1	–	–	–
Glc*p*	terminal	4	2	2	14	2	1	14
	4-	30	25	35	15	22	14	14
	6-	11	13	11	8	18	16	2
	4,6	13	12	15	18	20	15	28

[a] Terminal Ara*f* is deduced from 1,4-di-*O*-acetyl-2,3,5-tri-*O*-methylpentitol, etc.
[b] Average of duplicate determinations.
[c] –, Not detected.

digests from native and deacetylated xyloglucan. The digest of deacetylated xyloglucan thus contained a lower proportion of oligosaccharides in which the backbone Glc*p* residues were branched at O-6 of the non-reducing terminal Glc*p*.

In order to identify the differences between the digest of native and deacetylated xyloglucan, peaks N1 and N2 from the native digest (Fig. 2A) and peaks D1, D2 and D3 from the deacetylated digest (Fig. 2B) were collected and their linkage compositions analysed under basic conditions (Table 2). Linkage analysis of peaks N1 and N2 from the native digest contained 4-Glc*p*, 6-Glc*p*, and 4,6-Glc*p* in the approximate ratios 2:1:1 and 3:1:1, respectively (Table 2). These oligosaccharides thus contained two and three unbranched Glc*p* residues per molecule, respectively. Linkage analysis of peaks D1 and D2 from the digest of deacetylated xyloglucan contained 4-Glc*p*, 6-Glc*p* and 4,6-Glc*p* in the ratios 1:1:1 (Table 2). Thus, in contrast to the digest of native xyloglucan, the oligosaccharides, D1 and D2, from the digest of deacetylated xyloglucan contained only one unbranched Glc*p* residue per molecule, present as reducing 4-Glc*p*. Linkage analysis of peak D3 from the digest of deacetylated xyloglucan contained terminal Glc*p*, 4-Glc*p* and 4,6-Glc*p* in the ratios 1:1:2. Thus, this peak contained one reducing end-group 4-Glc*p* residue and one non-reducing terminal Glc*p* residue, and the linkage composition of this peak accounted for the differences in the relative proportions of 6-Glcp and 4,6-Glcp observed between the total endo-(1 → 4)-β-glucanase digests of the native and deacetylated xyloglucan.

The differences in the linkage analyses of the endo-(1 → 4)-β-glucanase digests of native and deacetylated xyloglucan, and their major peaks from anion-exchange HPLC, suggested that the digest of native xyloglucan contained oligosaccharides that had two

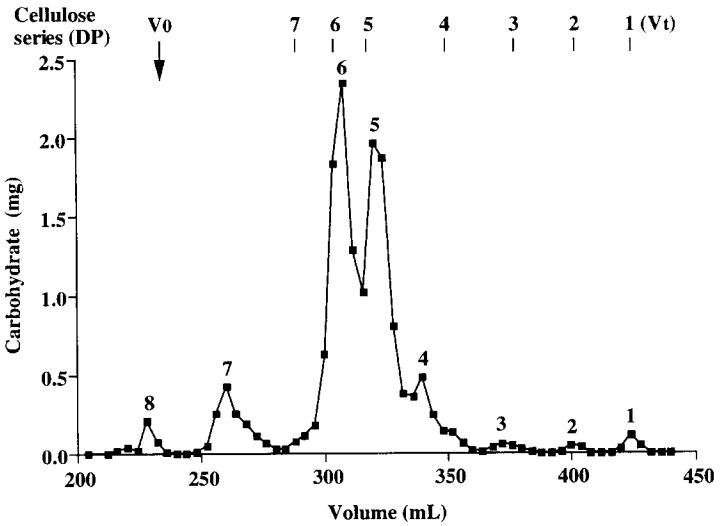

Fig. 3. Gel-filtration chromatography on a Fractogel TSK HW-40 column of native *Nicotiana plumbaginifolia* xyloglucan digested with endo-(1 → 4)-β-glucanase. The total carbohydrate content of each fraction (2 mL) was determined by the phenol–H_2SO_4 assay. The column was calibrated with a series of (1 → 4)-β-D-oligoglucosides (degree of polymerisation 1–7). Fractions (1–8) were collected for further analysis.

Table 3
Linkage composition of *Nicotiana plumbaginifolia* xyloglucan oligosaccharide fractions obtained by gel-filtration chromatography (Fig. 3). Samples were methylated under basic conditions with CH_3I, converted to partially methylated alditol acetates and analysed by GC–MS

Sugar	Deduced glycosidic linkage [a]	Linkage composition (mol%) [b]							
		Peak							
		1	2	3	4	5	6	7	8
Ara*f*	terminal	– [c]	–	9	18	17	13	14	16
Xyl*p*	terminal	–	1	7	17	14	14	9	14
	2-	–	–	6	15	13	11	15	17
Gal*p*	terminal	–	–	–	1	–	2	2	1
Glc*p*	terminal	100 [d]	61	26	2	1	2	1	2
	4-	–	37	38	21	26	30	30	22
	6-	–	1	14	18	16	12	7	12
	4,6-	–	–	–	8	14	17	22	18
Relative amount (% w/w) [e]		1	1	2	9	37	40	9	1

[a] Terminal Ara*f* is deduced from 1,4-di-*O*-acetyl-2,3,5-tri-*O*-methylpentitol, etc.
[b] Average of duplicate determinations.
[c] –, Not detected.
[d] Present as 90 mol% Glc*p* and 10 mol% Glc*f*, resulting from linkage analysis of free glucose.
[e] Calculated from total carbohydrate determinations of individual fractions.

Table 4

Quasimolecular ions from ESI–MS and relative proportions of oligosaccharides obtained from endo-(1 → 4)-β-glucanase digestion of native *Nicotiana plumbaginifolia* xyloglucan. Proportions of different peaks were from gel-filtration chromatography on a Toyopearl HW-40 column (Fig. 3). Proportions of individual oligosaccharides in peaks 3 and 4 were calculated from ESI–MS, and in peaks 5 and 6 calculated from anion-exchange HPLC (Fig. 4 and Table 6). These oligosaccharides account for 84% of the total endo-(1 → 4)-β-glucanase digest (the remaining material was composed of partially digested material (10%; Table 3) and oligosaccharides present in low proportions (6%))

Peak	(% w/w) of total digest	Pseudomolecular ion $[M+Na]^+$	Relative intensities (%)	Composition	Proposed glucosyl structure [a]	Relative amount (%) [a]	Relative abundance (%) [a]
1	1	n.d.	n.d.	n.d. [b]	G–	100	1
						100	
2	1	364.8	25	Hex_2	GG–	100	1
		407.4	75	Hex_2-OAc_1			
			100			100	
3	2	528.7	11	Hex_3	GGG–	51	1
		570.6	21	Hex_3-OAc_1			
		612.1	19	Hex_3-OAc_2			
		498.3	13	Hex_2Pent	XG–	15	tr
		540.5	2	$Hex_2Pent-OAc_1$			
		629.9	16	Hex_2Pent_2	SG–	34	< 1
		671.2	18	$Hex_2Pent_2-OAc_1$			
			100			100	
4	9	659.7	4	Hex_3Pent	XGG–	9	1
		701.7	4	$Hex_3Pent-OAc_1$			
		792.5	15	Hex_3Pent_2	XXG and/or SGG–	29	3
		834.6	15	$Hex_3Pent_2-OAc_1$			
		923.9	51	Hex_3Pent_3	SXG and/or XSG–	62	5
		966.4	11	$Hex_3Pent_3-OAc_1$			
			100			100	

5	37	953.7	3	Hex_4Pent_2	XXGG–	17	6
		996.3	10	$Hex_4Pent_2-OAc_1$			
		1038.4	4	$Hex_4Pent_2-OAc_2$			
		1087.0	8	Hex_4Pent_3	SXGG and/or XSGG–	56	21
		1128.4	38	$Hex_4Pent_3-OAc_1$			
		1169.8	10	$Hex_4Pent_3-OAc_2$			
		1218.0	4	Hex_4Pent_4	SSGG–	18	7
		1259.5	7	$Hex_4Pent_4-OAc_1$			
		1302.5	7	$Hex_4Pent_4-OAc_2$			
		Other	9		Other	9	3
			100			100	
6	40	1115.9	2	Hex_5Pent_2	XXGGG–	8	3
		1156.8	1	$Hex_5Pent_2-OAc_1$			
		1200.5	5	$Hex_5Pent_2-OAc_2$			
		1247.8	6	Hex_5Pent_3	SXGGG and XSGGG–	47	19
		1289.8	22	$Hex_5Pent_3-OAc_1$	XLXG and/or XXLG–	8	3
		1331.8	28	$Hex_5Pent_3-OAc_2$	X_2XGGG and/or XX_2GGG–	5	2
		1373.8	8	$Hex_5Pent_3-OAc_3$	GSXGG and/or GXSGG–	4	2
		1380.2	1	Hex_5Pent_4	SSGGG–	8	8
		1421.6	8	$Hex_5Pent_4-OAc_1$	GSSGG–	4	2
		1466.6	4	$Hex_5Pent_4-OAc_2$			
		1410.2	3	Hex_6Pent_3	XLLG–	8	3
		1452.2	2	$Hex_6Pent_3-OAc_1$			
		1494.3	2	$Hex_6Pent_3-OAc_2$			
		Other	8		Other	8	3
			100			100	
7 and 8	10	n.d.	n.d.	n.d.			10
	100						100

[a] After Fry et al. [7]; assignments and quantitations are for the glycosyl structures only, and quantitation using the ESI–MS data of isomeric forms generated by *O*-acetylation is only possible in fractions which contain only one structure.
[b] Not determined.

Table 5
Summary of ^{1}H chemical shifts for peak 5 from the gel-filtration column of *Nicotiana plumbaginifolia* xyloglucan digested with endo-(1 → 4)-β-glucanase

Residue	Chemical shift (ppm) [a]					
	H-1	H-2	H-3	H-4	H-5	H-6
α-D-Xylp_1	5.08 (3.4) [b]	3.57 (12.3)	3.84	– [c]	–/–	
α-D-Xylp_2	5.05 (3.7)	3.56 (12.3)	3.83		–/–	
α-D-Xylp_{ter1}	4.95 (4.1)	3.54	3.71	–	–/–	
α-D-Xylp_{ter2}	4.93 (3.6) [b]	3.54	3.71	–	–/–	
α-L-Araf_1 (*O*-acetyl)	5.17	4.20	4.01	–	4.39/–	
α-L-Araf_2	5.16	4.19	3.92	4.08	3.83/3.70	
α-L-Araf_3	5.15	4.19	3.91	4.05	3.82/3.69	
red. α-D-Glcp_1	5.21	3.57	3.77 (5.1)	–	–	–/–
red. β-D-Glcp_1	4.64 (8.1) [b]	3.27	3.62	–	–	3.81/3.93
β-D-Glcp_2 (*O*-acetyl)	4.54	3.37	3.66	3.76	3.84	4.30/4.60 (12.3)

[a] Chemical shifts measured relative to Me_2SO as 2.71 ppm [30].
[b] Coupling constants (Hz) which could be easily measured from the 1D spectrum or slices of the 2D TOCSY are included.
[c] Resonances for these peaks are in heavily overlapped regions and could not be assigned.

and three contiguous Glc*p* residues that were not branched to Xyl*p* residues. This was further substantiated by the increase in glucose and cellobiose in the digest of deacetylated xyloglucan, which could only be produced if the polysaccharide contained two or three contiguous unbranched Glc*p* residues, respectively. Further, a comparison of the endo-glucanase digestion of native and deacetylated xyloglucan suggested that the enzyme did not cleave glycosidic linkages involving the anomeric carbon of 4-Glc*p* residues *O*-acetylated at C-6, and suggests that the reducing 4-Glc*p* residues at the sites of cleavage in the native xyloglucan were not acetylated. Based upon these data and the desire to determine the positions of both glycosyl and non-glycosyl substituents on the (1 → 4)-β-glucan backbone of the xyloglucan, it was decided to digest native xyloglucan with endo-(1 → 4)-β-glucanase and separate by oligosaccharides by a combination of gel-filtration chromatography and anion-exchange HPLC.

Chromatography of xyloglucan oligosaccharides.—Gel-filtration chromatography on a Fractogel TSK HW-40 column of the ethanol-soluble products from *N. plumbaginifolia* native xyloglucan digested with endo-glucanase for 8 h gave 8 peaks (Fig. 3). Peaks 1–6 were collected and the primary structure of the oligosaccharides determined by a combination of linkage analysis (Table 3) and ESI–MS (Table 4). Peak 7 (> 3000 amu from ESI–MS), which accounted for 9% of the total digest and peak 8 (eluting at the V_0 of the column), which accounted for 1% of the total digest, contained partially digested material; they were not analysed further. Peak 5, which comprised 37% (w/w) of the total digest, was also analysed by ^{1}H-NMR (Table 5). Peaks 5 and 6, which comprised 77% (w/w) of the oligosaccharide material, were further fractionated by anion-exchange HPLC (Fig. 4), and the structures of the individual oligosaccharides determined by linkage analysis (Table 6) and ESI–MS.

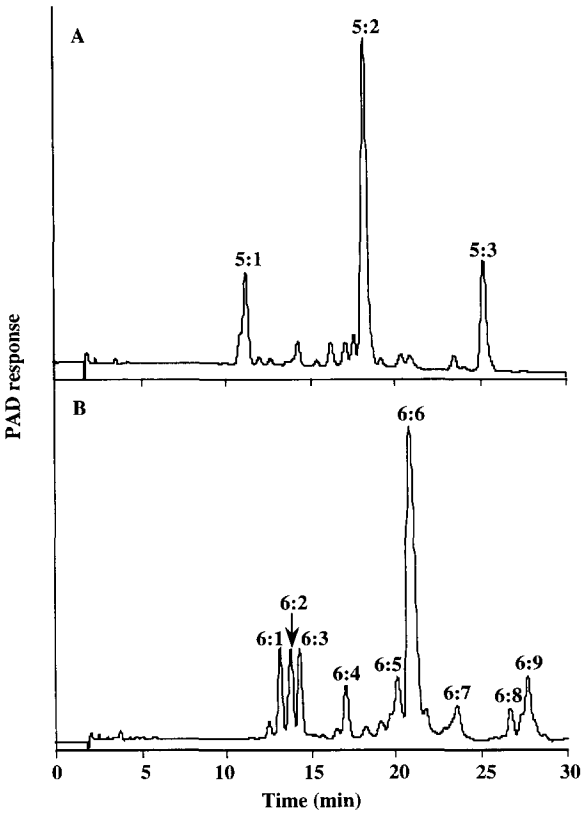

Fig. 4. Anion-exchange HPLC of peak 5 (A) and peak 6 (B) from gel-filtration chromatography (Fig. 3) of native *Nicotiana plumbaginifolia* xyloglucan digested with endo-(1 → 4)-β-glucanase. The oligosaccharides were separated on a CarboPac PA-1 column equilibrated in 150 mM NaOH containing 60 mM NaOAc and eluted with a 40 min linear gradient of NaOAc (60–250 mM) starting 5 min after sample injection. The eluted material was detected by pulsed amperometric detection. The fractions indicated were collected and deionised in preparation for linkage analysis and ESI–MS.

Structure of peaks 1 and 2.—Peaks 1 and 2 each constituted 1% (w/w) of the endo-(1 → 4)-β-glucanase digest of native xyloglucan. Linkage analysis of these peaks, which co-chromatographed on the gel-filtration column with glucose and cellobiose, showed that peak 1 contained only terminal Glc (90 mol% Glc*p* and 10 mol% Glc*f*, resulting from linkage analysis of free glucose) and that peak 2 contained predominantly terminal Glc*p* and 4-Glc*p* (Table 3). The ratio of terminal Glc*p* and 4-Glc*p* in peak 2 was 1:0.6, slightly less than the 1:1 expected for cellobiose. A pseudomolecular ion $[M + Na]^+$ in the ESI–MS spectrum of native peak 2 at *m/z* 365 corresponded to Hex_2 (namely cellobiose; Table 4). A second pseudomolecular ion at *m/z* 407 corresponded to Hex_2 with an *O*-acetyl group attached; the relative abundance of the two pseudomolecular ions suggested that 75% of the cellobiose was monoacetylated. Since endo-(1 → 4)-

β-glucanase does not appear to cleave the glycosidic linkage involving the anomeric carbon of *O*-acetylated 4-Glc*p* residues (see above), the site of *O*-acetylation on cellobiose must be on C-6 of the non-reducing terminal Glc*p* residue (i.e. Ac*O*-6-Glc*p*-(1 → 4)-β-Glc*p*).

Structure of peak 3.—Peak 3 from the gel-filtration column comprised only 2% (w/w) of the total endo-(1 → 4)-β-glucanase digest. Linkage analysis showed that it contained mostly terminal Glc*p*, 4-Glc*p*, and 6-Glc*p*, with smaller amounts of terminal Xyl*p* and 2-Xyl*p* and terminal Ara*f* (Table 3). ESI–MS yielded pseudomolecular ions corresponding to Hex_3–OAc_{0-2}, Hex_2Pent–OAc_{0-1} and Hex_2Pent_2–OAc_{0-1}, respectively (Table 4). The relative abundances of the *O*-acetylated species varied with the structure of the oligosaccharides, and in addition to mono-*O*-acetylated species, Hex_3 was also di-*O*-acetylated (Table 4). From the ESI–MS and the linkage analysis it was deduced that peak 3 was composed of GGG (**3:1**; 51%), XG (**3:2**; 15%), and SG (**3:3**; 34%). The sites of *O*-acetylation were assigned from the susceptibility of the xyloglucan to the endo-(1 → 4)-β-glucanase (see above), and on **3:1** were deduced to be on C-6 of one or both of the non-reducing Glc*p* residues, and on **3:3** on C-5 of the terminal Ara*f* residue. Only a small proportion (12%) of **3:2** was *O*-acetylated, but the site of *O*-acetylation was not identified. However, from the action pattern of the endo-(1 → 4)-β-glucanase, the *O*-acetyl substituent could not have been present at C-6 of the reducing 4-Glc*p* residue, suggesting it can only be present on the terminal Xyl*p* residue, although this was not detected in the linkage analysis of xyloglucan under neutral conditions (see above).

Table 6
Linkage composition of *Nicotiana plumbaginifolia* xyloglucan oligosaccharides present in peaks 5 and 6 (Fig. 3) after anion-exchange HPLC (Fig. 4). Samples were methylated under basic conditions with CH_3I, converted to partially methylated alditol acetates and analysed by GC–MS

Sugar	Deduced glycosidic linkage [a]	Linkage composition (mol%) [b]											
		Fraction											
		5:1	5:2	5:3	6:1	6:2	6:3	6:4	6:5	6:6	6:7	6:8	6:9
Ara*f*	terminal	– [c]	13	25	–	–	–	–	14	11	15	23	25
Xyl*p*	terminal	37	19	–	25	12	25	24	12	15	14	–	–
	2-	–	13	22	11	17	4	10	9	11	9	18	19
Gal*p*	terminal	–	–	–	12	23	5	–	–	–	–	–	–
Glc*p*	terminal	3	3	2	2	–	1	–	9	2	1	14	1
	4-	30	25	25	16	18	37	44	35	35	40	22	33
	6-	14	13	13	11	11	11	11	6	11	9	31	0
	4,6-	16	13	13	23	19	17	11	15	15	11	19	11
Relative amount (%w/w) [d]		16	56	18	8	8	8	5	4	42	5	4	8

[a] Terminal Ara*f* is deduced from 1,4-di-*O*-acetyl-2,3,5-tri-*O*-methylpentitol, etc.
[b] Average of duplicate determinations.
[c] –, Not detected.
[d] Calcluated from peak areas from anion-exchange HPLC, assuming an equimolar response for each.

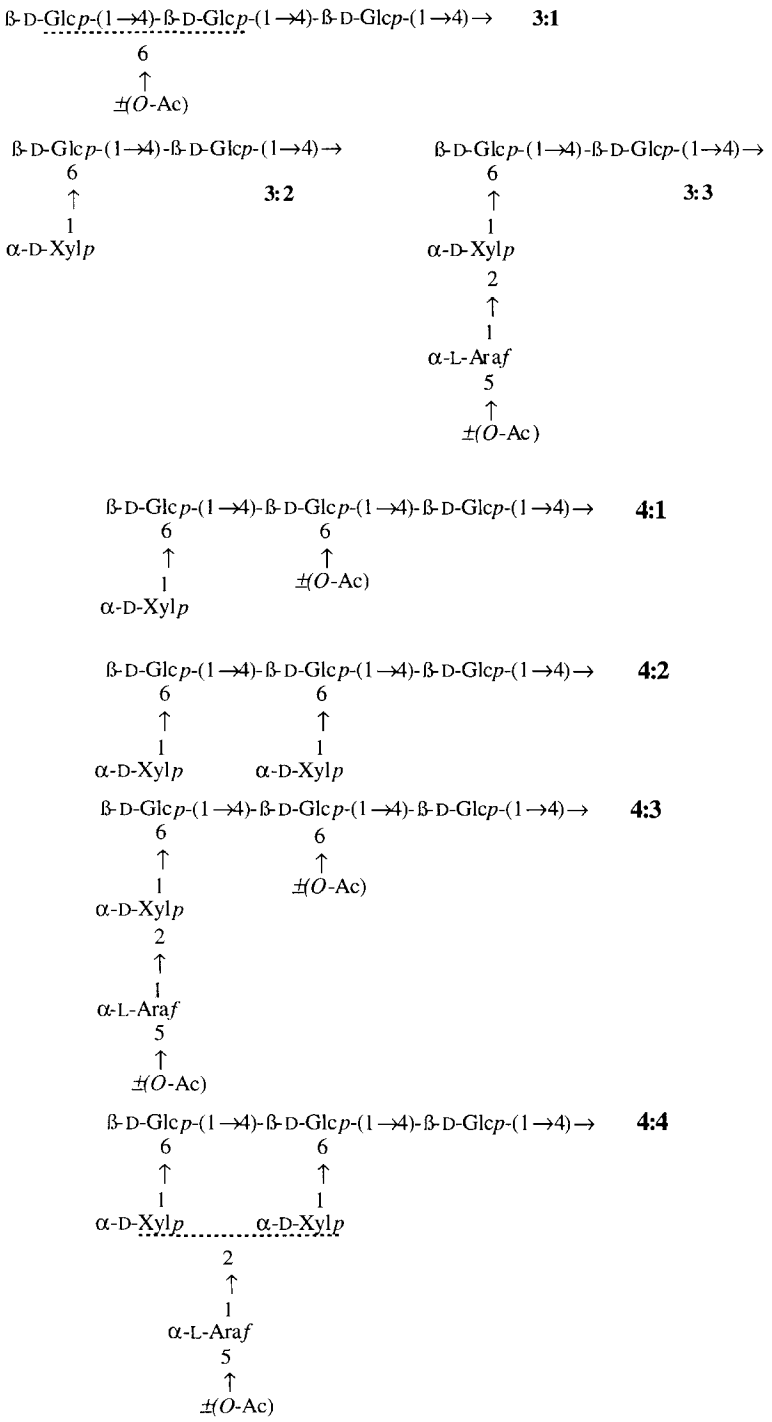
ß-D-Glcp-(1→4)-ß-D-Glcp-(1→4)-ß-D-Glcp-(1→4)→ 3:1
6
↑
±(O-Ac)
ß-D-Glcp-(1→4)-ß-D-Glcp-(1→4)→
6
↑
1
α-D-Xylp
3:2
ß-D-Glcp-(1→4)-ß-D-Glcp-(1→4)→
6
↑
1
α-D-Xylp
2
↑
1
α-L-Araf
5
↑
±(O-Ac)
3:3
ß-D-Glcp-(1→4)-ß-D-Glcp-(1→4)-ß-D-Glcp-(1→4)→ 4:1
6 6
↑ ↑
1 ±(O-Ac)
α-D-Xylp
ß-D-Glcp-(1→4)-ß-D-Glcp-(1→4)-ß-D-Glcp-(1→4)→ 4:2
6 6
↑ ↑
1 1
α-D-Xylp α-D-Xylp
ß-D-Glcp-(1→4)-ß-D-Glcp-(1→4)-ß-D-Glcp-(1→4)→ 4:3
6 6
↑ ↑
1 ±(O-Ac)
α-D-Xylp
2
↑
1
α-L-Araf
5
↑
±(O-Ac)
ß-D-Glcp-(1→4)-ß-D-Glcp-(1→4)-ß-D-Glcp-(1→4)→ 4:4
6 6
↑ ↑
1 1
α-D-Xylp α-D-Xylp
2
↑
1
α-L-Araf
5
↑
±(O-Ac)

Structure of peak 4.—Peak 4 from the gel-filtration column comprised 9% (w/w) of the total endo-(1 → 4)-β-glucanase digest. Linkage analysis detected mostly 4-Glc*p*, 6-Glc*p*, and 4,6-Glc*p*, terminal Xyl*p* and 2-Xyl*p* and terminal Ara*f* (Table 3). ESI–MS yielded pseudomolecular ions which corresponded to oligosaccharides with Hex_3Pent–OAc_{0-1}, Hex_3Pent_2–OAc_{0-1} and Hex_3Pent_3–OAc_{0-1} (Table 4). Thus, it was deduced that peak 4 contained XGG (**4:1**; 9%), XXG (**4:2**) and/or SGG (**4:3**; 29%), and SXG and/or XSG (**4:4**; 62%). From the susceptibility of the xyloglucan to the endo-glucanase, the site of *O*-acetylation on **4:1** and **4:3** was deduced to be C-6 of the internal 4-Glc*p* residues, although we cannot exclude the possibility that the *O*-acetyl group on **4:3** is attached to C-5 of the terminal Ara*f* residue. Structure **4:4** was deduced to be *O*-acetylated only on C-5 of the terminal Ara*f* residue.

Structure of peak 5.—Peak 5 from the gel-filtration column comprised 37% (w/w) of the total endo-(1 → 4)-β-glucanase digest. Linkage analysis showed that peak 5 contained 4-Glc*p*, 6-Glc*p*, and 4,6-Glc*p*, terminal Xyl*p*, and 2-Xyl*p*, and terminal Ara*f* in the approximate molar ratios 2:1:1:1:1:1 (Table 3), which corresponded to the average molecular structure being SXGG and/or XSGG. However, ESI–MS yielded pseudomolecular ions which corresponded to the presence of three separate oligosaccharides with Hex_4Pent_2–OAc_{0-2}, Hex_4Pent_3–OAc_{0-2} and Hex_4Pent_4–OAc_{0-2} (Table 4).

Anion-exchange HPLC of gel-filtration peak 5 (Fig. 3) yielded three major individual oligosaccharides, 5:1 (16% w/w), 5:2 (56% w/w), and 5:3 (18% w/w) together with several minor components (< 3% w/w each of total) which were not collected for analysis (Fig. 4A and Table 6). Linkage analysis showed that these fractions contained 4-Glc*p*, 6-Glc*p*, and 4,6-Glc*p* in the approximate molar ratio of 2:1:1, indicating that each of the oligosaccharides were composed of two branched and two unbranched Glc*p* residues (Table 6). In addition to the Glc*p*, fraction 5:1 also contained terminal Xyl*p*, and ESI–MS yielded a pseudomolecular ion at *m/z* 952.8 corresponding to Hex_4Pent_2; fraction 5:2 also contained terminal Xyl*p*, 2-Xyl*p* and terminal Ara*f*, and ESI–MS gave a pseudomolecular ion at *m/z* 1086.2 corresponding to Hex_4Pent_3; fraction 5:3 also contained 2-Xyl*p* and terminal Ara*f* and ESI–MS gave a pseudomolecular ion at *m/z* 1217.4 corresponding to Hex_4Pent_4. The three oligosaccharides from peak 5 were thus identified as XXGG (**5:1**), SXGG and/or XSGG (**5:2**), and SSGG (**5:3**), respectively.

^{1}H-NMR spectra were acquired on a sample of peak 5 from the gel-filtration column which included all three oligosaccharides (**5:1**, **5:2** and **5:3**) and their *O*-acetylated derivatives. The ^{1}H chemical shifts for three Glc ring systems, four Xyl ring systems, and three Ara systems are given in Table 5. The assignments were based on comparison of these chemical shifts with those of similar xyloglucan oligosaccharides [8,15,31] and standard chemical shift data for monosaccharides [32]. The 1D spectrum was complex and contained many overlapping signals, but showed 8 anomeric peaks of varying intensities, downfield from HOD. Following 2D analysis, these peaks were assigned as reducing α-D-Glc (designated red. α-D-Glc_1; confirmed by the disappearance of this peak upon reduction of the sample with $NaBH_4$ [15]), 4 different Xyl*p* ring systems (α-D-$Xylp_1$, α-D-$Xylp_2$, α-D-$Xylp_{ter1}$, and α-D-$Xylp_{ter2}$, in order of their descending chemical shifts (δ)) and three Ara*f* ring systems (α-L-$Araf_1$, α-L-$Araf_2$, and α-L-$Araf_3$). The assignments of the three Ara*f* ring systems were based on comparison of the chemical shifts with those of Ara*f* from arabinogalactan–protein [30], and were consis-

tent with there being only terminal Ara*f*. However, the chemical shift for H-5 of α-L-Araf_1 was markedly different to α-L-Araf_2 and α-L-Araf_3, being 0.60 ppm downfield from H-5 in α-L-Araf_3. A smaller downfield change was also noted for H-3 of α-L-Araf_1 compared with α-L-Araf_2 and α-L-Araf_3. This trend suggested that the C-5 on a proportion of the terminal Ara*f* residues were *O*-acetylated, and supported the data from the methylation analyses under neutral conditions (Table 1), the susceptibility of xyloglucan to the endo-(1 → 4)-β-glucanase, and the ESI–MS data (Table 4). Such a deshielding effect on δ is common for protons attached to a carbon atom substituted with an *O*-acetyl group [8,31].

Upfield of the water peak the anomeric region was overlapped, and individual peaks could not be identified until a full 2D analysis had been completed. In the 2D TOCSY, the anomeric proton at δ 4.64 ppm was assigned to the reducing β-D-Glc*p* residues (designated red. β-D-Glc$_1$ in Table 5; confirmed by the disappearance of this peak upon reduction of the sample with $NaBH_4$ [15]). The anomeric protons of the other Glc*p* residues were very similar, all having δ values between 4.45–4.57 ppm. One of the overlapped Glc*p* residues showed strong TOCSY correlations to two H-6 protons within the anomeric region (δ of 4.30 and 4.60 ppm), and this connectivity allowed the unambiguous assignment of the remainder of this spin system (β-D-Glcp_2 in Table 5). The downfield shift of the H-6 protons is due to *O*-acetylation on C-6; taken together with the specificity of the endo-(1 → 4)-β-glucanase, we can conclude that these *O*-acetyls are on the 4-Glc*p* residues proximal to the reducing 4-Glc*p* residues. The ESI–MS data (Table 4) indicated that all three oligosaccharides had up to two *O*-acetyl groups, indicating that in **5:1** at least, a small proportion of the 4-Glc*p* residues may be di-*O*-acetylated. The spectral data obtained for peak 5 from the gel-filtration column gave important insights into the composition and structure of the oligosaccharides, although isolation of the individual components in their native state would enable a more complete assignment and characterisation using ^{1}H-NMR spectroscopy to be conducted.

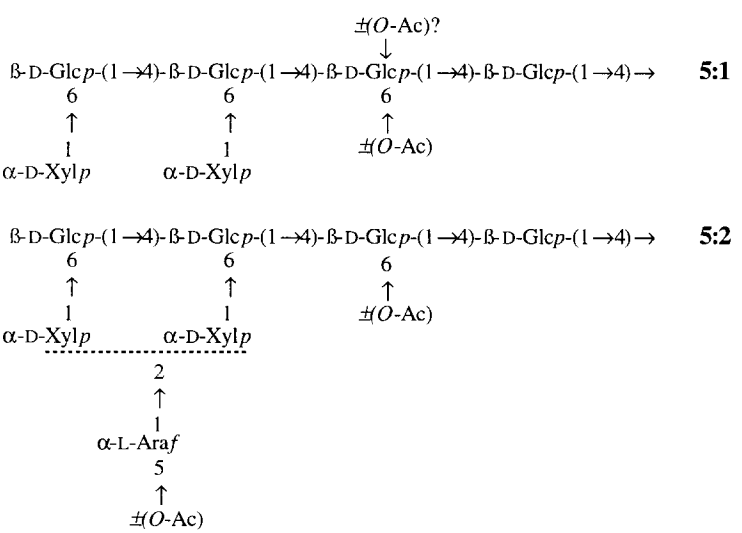

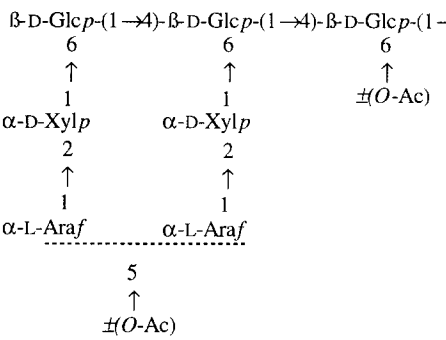

5:3

Structure of peak 6.—Peak 6 from the gel-filtration column comprised 40% (w/w) of the total endo-(1 → 4)-β-glucanase digest. The linkage composition was similar to that of peak 5, but also contained a small amount of terminal Gal*p* (2 mol%; Table 3). ESI–MS of native peak 6 gave a complex series of pseudomolecular ions, which corresponded to Hex_5Pent_2–OAc_{0-2}, Hex_5Pent_3–OAc_{0-3}, Hex_5Pent_4–OAc_{0-2} and Hex_6Pent_3–OAc_{0-2} (Table 4).

The anion-exchange HPLC profile of HW-40 gel-filtration peak 6 (Fig. 3) was more complex than peak 5, and yielded 9 major individual oligosaccharides, 6:1 (8% w/w), 6:2 (8%), 6:3 (8%), 6:4 (5%), 6:5 (4%), 6:6 (42%), 6:7 (5%), 6:8 (4%) and 6:9 (8%; Fig. 4B and Table 6). Oligosaccharides present in minor amounts (< 2% w/w) were not collected for analysis. The linkage compositions of fractions 6:1 and 6:2 were similar, with each fraction containing 4-Glc*p*, 6-Glc*p*, and 4,6-Glc*p*, terminal Xyl*p* and 2-Xyl*p* and terminal Gal*p* (Table 6). However, fraction 6:2 contained half as much terminal Xyl*p* and twice as much terminal Gal*p* as fraction 6:1. ESI–MS of these two oligosaccharides gave pseudomolecular ions at *m/z* 1247.7 and 1409.9, corresponding to Hex_5Pent_3 and Hex_6Pent_3, respectively. From comparison with the structures of oligosaccharides obtained by endo-glucanase digestion of tamarind xyloglucan [31], fraction 6:1 was deduced to be XLXG and/or XXLG (**6:1**), and fraction 6:2 was deduced to be XLLG (**6:2**). ESI–MS (Table 4) indicated that one or two *O*-acetyl groups were present on a proportion of both of these molecules; since no *O*-acetylated Xyl*p* residues were detected by linkage analysis under neutral conditions (Table 1) and the reducing 4-Glc*p* residues cannot be *O*-acetylated based on the specificity of the endo-(1 → 4)-β-glucanase, these *O*-acetyl groups were probably located on the terminal Gal*p* residues, similar to that which was reported for 2-Gal*p* residues in xyloglucan secreted by *A. pseudoplatanus* suspension cultures [15].

The linkage composition of fraction 6:3 yielded predominantly 4-Glc*p*, 6-Glc*p*, and 4,6-Glc*p* and terminal Xyl*p* (Table 6) and ESI–MS gave a major pseudomolecular ion at *m/z* 1114.8 (83%) corresponding to Hex_5Pent_2 and a minor pseudomolecular ion at *m/z* 1409.6 (17%) corresponding to Hex_6Pent_3. Fraction 6:3 was identified as XXGGG (**6:3**), and the presence of low levels of 2-Xyl*p* and terminal Gal*p* in the linkage analyses and a pseudomolecular ion with *m/z* 1409.6 in the ESI spectrum was deduced to result from carry over from fraction 6:2. *O*-Acetyl groups were deduced to be present on C-6 of one or both of a proportion of the internal 4-Glc*p* residues.

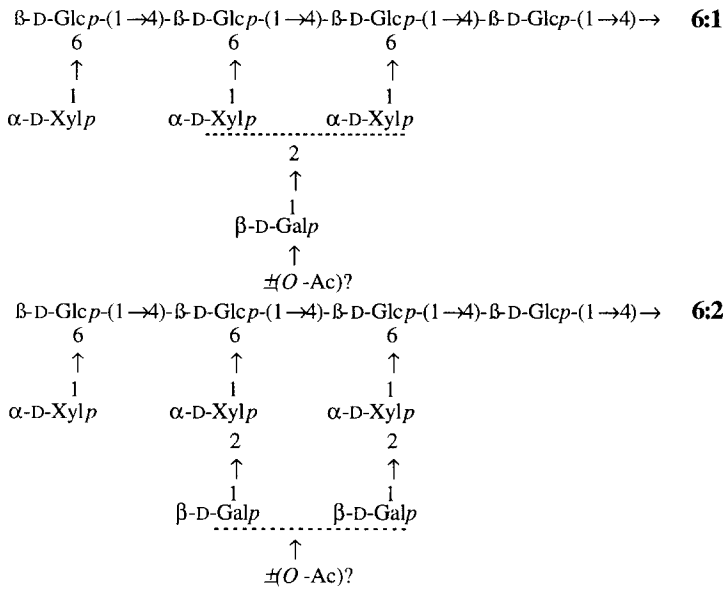

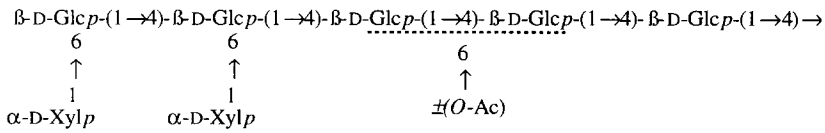

6:3

The linkage composition of fraction 6:4 contained similar proportions of 4-Glc*p*, 6-Glc*p*, and 4,6-Glc*p*, and terminal Xyl*p* to that of fraction 6:3 (Table 6) but, contained higher levels of 2-Xyl*p* (10 mol%) and no terminal Gal*p*. ESI–MS gave a major pseudomolecular ion with *m/z* 1247.3 corresponding to Hex_5Pent_3. This fraction was thus deduced to be X_2XGGG and/or XX_2GGG (**6:4**), with one of the 4,6-Glc*p* residues substituted with terminal Xyl*p* and the other substituted with Xyl*p*-(1 → 2)-Xyl*p*. *O*-Acetyl groups were deduced to be present on C-6 of one or both of a proportion of the internal 4-Glc*p* residues.

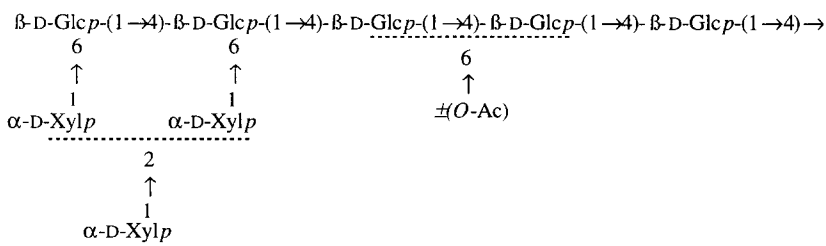

6:4

The linkage analyses of fractions 6:5, 6:6, and 6:7 contained similar amounts of terminal Ara*f*, terminal Xyl*p* and 2-Xyl*p* (Table 6). Fractions 6:6 and 6:7 also contained similar proportions of 4-Glc*p*, 6-Glc*p*, and 4,6-Glc*p*, whereas fraction 6:5 contained less 6-Glc*p* and more terminal Glc*p* than these two fractions. ESI–MS of these three fractions gave pseudomolecular ions at *m/z* 1247.7, 1247.6, and 1247.8, respectively, which corresponded to Hex_5Pent_3. Fraction 6:5 was deduced to contain ~60% GXSGG and/or GSXGG (**6:5**), but the presence of 6-Glc*p* (Table 6) indicated that this fraction also contained material carried over from fraction 6:6. Fractions 6:6 and 6:7 were deduced to be SXGGG and XSGGG (**6:6**), although the precise identity of each peak was not investigated. *O*-Acetyl groups were deduced to be present mostly on C-6 of a proportion of the terminal Glc*p* and internal 4-Glc*p* residues of **6:5**, and mostly on C-6 of a proportion of one or both of the internal 4-Glc*p* residues of **6:6**. ESI–MS of fraction 6 (Table 4) gave a pseudomolecular ion corresponding to Hex_5Pent_3–OAc_3 which suggested that a small proportion (13%) of these oligosaccharides were tri-*O*-acetylated. In this case, two *O*-acetyl groups were probably present on the Glc*p* backbone, with a third *O*-acetyl group located on terminal Ara*f*.

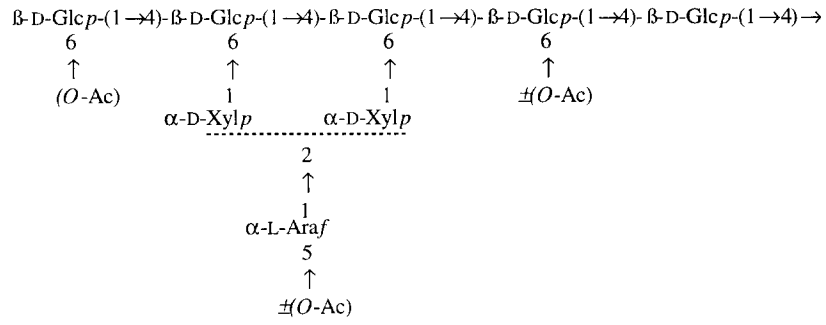

6:5

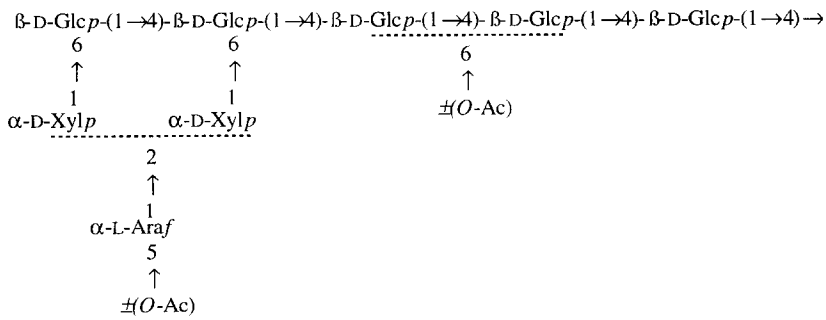

6:6

Fractions 6:8 and 6:9 contained terminal Ara*f* and 2-Xyl*p* in similar proportions, but different proportions of terminal Glc*p*, 4-Glc*p*, 6-Glc*p*, and 4,6-Glc*p*. Fraction 6:8 contained 14 mol% terminal Glc*p* and only 3 mol% 6-Glc*p* suggesting that the major

oligosaccharide in this fraction was not branched at O-6 of the non-reducing terminal Glc*p* to a Xyl*p* residue. In contrast, fraction 6:9 contained only 1 mol% terminal Glc*p* and 10 mol% 6-Glc*p*, indicating that the major oligosaccharide was branched at O-6 of the non-reducing terminal Glc*p* to a Xyl*p* residue. ESI–MS of these fractions gave pseudomolecular molecular ions at m/z 1379.7 and 1379.6, respectively, corresponding to Hex_5Pent_4. Fractions 6:8 and 6:9 were thus deduced to be GSSGG (**6:7**) and SSGGG (**6:8**), respectively. *O*-Acetyl groups were deduced to be present on C-6 of a proportion of the non-reducing terminal Glc*p* and internal 4-Glc*p* residues of **6:7**, and on C-6 of a proportion of one or both of the internal 4-Glc*p* residues of **6:8**. *O*-Acetyl groups were probably also present on C-5 of a proportion of one or both of the terminal Ara*f* residues of each in these oligosaccharides.

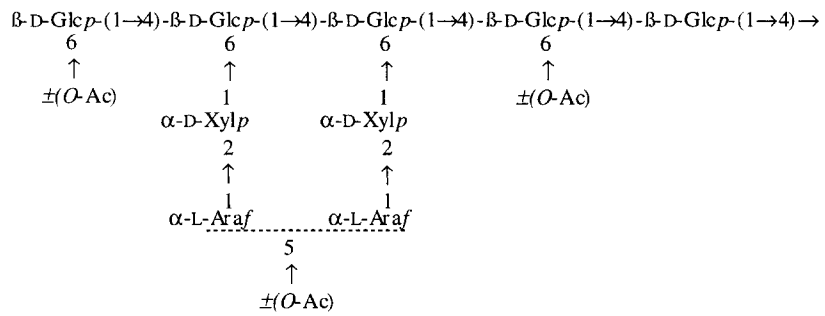

6:7

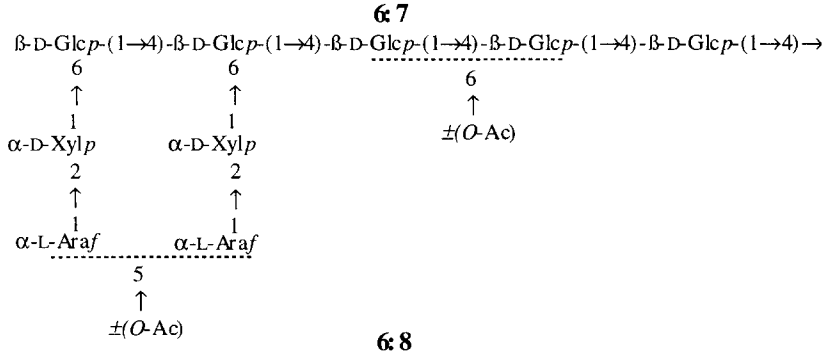

6:8

4. Conclusions

Xyloglucan from *N. plumbaginifolia* cell-suspension cultures has a similar primary structure to that from *N. tabacum* leaves and suspension cultures [9,33]. The xyloglucan has a backbone of (1 → 4)-β-D-Glc*p* residues of which ~ 40% are branched at O-6 to α-Xyl*p*, or α-L-Ara*f*-(1 → 2)-α-Xyl*p*, or β-D-Gal*p*-(1 → 2)-α-Xyl*p*, or α-D-Xyl*p*-(1 → 2)-α-Xyl*p*. The relative proportions of the different oligosaccharides present in endo-(1

→ 4)-β-glucanase digests of native *N. plumbaginifolia* xyloglucan is summarised in Table 4. The majority of the xyloglucan is composed of oligosaccharides based on the subunits XXGG (34%) and XXGGG (27%; Table 4). Almost 60% of the oligosaccharide subunits are further substituted with one terminal Ara*f* residue, and almost 15% are substituted with two terminal Ara*f* residues attached at O-2 of the Xyl*p* residues. Most of the remaining subunits are not substituted with terminal Ara*f* residues, although a small proportion (~ 2%) are substituted with terminal Xyl*p* residues attached at O-2 of the Xyl*p* residues (structure **6:4**). In addition, *N. plumbaginifolia* xyloglucan also contains a low proportion (~ 6% of the total endo-(1 → 4)-β-glucanase digest) of oligosaccharides which are substituted at C-6 of 75% of the 4-Glc*p* backbone and contain side-chains composed of α-D-Xyl*p* and Gal*p*(1 → 2)-α-Xyl*p*, similar to tamarind seed xyloglucan (structures **6:1** and **6:2)** [31]. These oligosaccharides may represent a separate xyloglucan present in a low proportion, or may be a minor substitution pattern on a single molecule. Xyloglucan from *S. tuberosum* contains approximately equal amounts of terminal Ara*f* and terminal Gal*p* [11]. However, *N. plumbaginifolia* xyloglucan contains some 15 times more terminal Ara*f* than terminal Gal*p*.

The major subunit of xyloglucan isolated from cell walls of *N. tabacum* with alkali was XXG with single Ara*f* residues attached [10]. Gel-filtration chromatography of their endo-glucanase digested *N. tabacum* xyloglucan showed that a significant amount of glucose and cellobiose was present. Similarly, in the present study, alkali-treated, deacetylated *N. plumbaginifolia* xyloglucan digested with endo-(1 → 4)-β-glucanase also produced considerable amounts of glucose and cellobiose, and yielded oligosaccharides based on XXG as the major products. Thus, it is probable that xyloglucans from *N. plumbaginifolia* and *N. tabacum* have similar structures.

The *N. plumbaginifolia* xyloglucan contained *O*-acetyl groups attached mostly to the C-6 of 4-Glc*p* residues which were not substituted with Xyl*p*, and less commonly to C-5 of some of the terminal Ara*f* residues. Approximately 30% of the 4-Glc*p* backbone residues were *O*-acetylated, which was equivalent to 44% of the 4-Glc*p* residues not xylosylated, and approximately 15% of the terminal Ara*f* residues were *O*-acetylated. Comparison of the endo-glucanase digests of native and deacetylated xyloglucan suggests that cleavage sites in the native xyloglucan are at glycosidic linkages involving the anomeric carbon of 4-Glc*p* residues that are not *O*-acetylated, and from the pattern of oligosaccharides obtained, it appears that the distribution of *O*-acetyl groups on the Glc*p* backbone is not random. Substitution of the backbone of other solanaceous xyloglucans with *O*-acetyl groups has been reported recently [16], although this present study represents the first detailed investigation of the degree of *O*-acetylation and is the first time that *O*-acetylation has been reported on terminal Ara*f* residues. *O*-Acetylation has been reported at C-3, C-4 and C-6 of the 2-Gal*p* residues present in side-chains of xyloglucan isolated from cell-suspension cultures of *A. pseudoplatanus* [15], whereas *O*-acetylation was predominantly at C-6 of the 4-Glc*p* residues and at C-5 of the terminal Ara*f* residues in *N. plumbaginifolia* xyloglucan, although it appears that the rare terminal Gal*p* residues may also be *O*-acetylated (structures **6:1** and **6:2**). Further, *N. plumbaginifolia* xyloglucan contained glycosyl residues which were primarily mono-*O*-acetylated (> 95%), whereas 25–30% of the glycosyl residues in *A. pseudoplatanus* xyloglucan contained residues which were di-*O*-acetylated. Thus, the pattern *O*-acetyla-

tion was relatively homogeneous in *N. plumbaginifolia* xyloglucan, and contrasted with the heterogeniety of *O*-acetylation in xyloglucan from *A. pseudoplatanus*.

The role of *O*-acetylation of xyloglucans is not understood and further work is required to identify its biological function. It has been suggested that enzymic removal of *O*-acetyl groups from the 2-Gal*p* residues present in side-chains may direct association, via hydrogen-bonding, of the open face xyloglucan to cellulose [4]. In xyloglucan secreted into the medium of suspension cultures of *N. tabacum*, it has been suggested that the *O*-acetyl and glycosidic substitution patterns of the backbone may maintain a molecular topology required for formation of a xyloglucan/cellulose network in cell walls [16]. In *N. plumbaginifolia*, it is unclear whether *O*-acetylation of the glucose backbone maintains a conformation of the secreted xyloglucan which enables it to hydrogen bond to cellulose, or whether removal of *O*-acetyl groups is necessary for association of xyloglucan and cellulose. The location of *O*-acetyl groups on the backbone may also affect the accessibility of xyloglucan to cell wall enzymes. *O*-Acetylation may reduce the ability of xyloglucan chains to act as a substrate for xyloglucan endotransglycosylase (XET), and, in addition to exo-glycosylhydrolases, an esterase might also play a role in the control of the action of XET [34]. In the present study, *O*-acetylation of xyloglucan secreted into the extracellular medium of *N. plumbaginifolia* suspension-cultures has been shown to block the action of endo-(1 → 4)-β-glucanase and α-L-arabinofuranosidase. Similarly, *O*-acetylation of xyloglucan within the walls of these cells may reduce its susceptibility to XET [34], and thus play a role in controlling cell wall expansion. It would be interesting to determine the degree and pattern of *O*-acetylation on xyloglucan in walls of *N. plumbaginifolia* cells throughout wall expansion.

Acknowledgements

We wish to thank Dr. David McManus for the production and supply of ECPs from *N. plumbaginifolia*, Dr. Alison Gane for analysis of acetic acid, and Dr. Steve Read for critical assessment of the manuscript. This research was supported by funds from a Cooperative Research Centre Program of the Commonwealth Government of Australia to the CRC for Industrial Plant Biopolymers, and the ESI–MS was purchased with grants from the University of Melbourne, the Australian Research Council, the Clive and Vera Ramaciotti Foundation and the Ian Potter Foundation.

References

[1] M. McNeil, A.G. Darvill, S. Fry, and P. Albersheim, *Ann. Rev. Biochem.*, 53 (1984) 625–663.
[2] S.C. Fry, *J. Exp. Bot.*, 40 (1989) 1–11.
[3] T. Hayashi, *Ann. Rev. Plant Physiol. Plant Mol. Biol.*, 40 (1989) 139–168.
[4] N.C. Carpita and D.M. Gibeaut, *Plant J.*, 3 (1993) 1–30.
[5] A. Darvill, M. McNeil, P. Albersheim, and D.P. Delmer, in N.E. Tolbert (Ed.), *The Biochemistry of Plants*, Vol. 1, Academic Press, New York, 1980, pp 92–162.

[6] A. Bacic, P.J. Harris, and B.A. Stone, in J. Priess (Ed.), *The Biochemistry of Plants, A Comprehensive Treatise*, Vol. 14, Academic Press, New York, 1988, pp 297–371.
[7] S.C. Fry, W.S. York, P. Albersheim, A. Darvill, T. Hayashi, J.-P. Joseleau, Y. Kato, P. Lorences, G.A. Maclachlan, M. McNeil, A.J. Mort, J.S.G. Reid, H.U. Seitz, R.R. Selvendran, A.G.J. Voragen, and A.R. White, *Physiol. Plant.*, 89 (1993) 1–3.
[8] W.S. York, H. van Halbeek, A.G. Darvill, and P. Albersheim, *Carbohydr. Res.*, 200 (1990) 9–31.
[9] S. Eda and K. Kato, *Agric. Biol. Chem.*, 42 (1978) 351–357.
[10] M. Mori, S. Eda, and K. Kato, *Agric. Biol. Chem.*, 43 (1979) 145–149.
[11] S.G. Ring and R.R Selvendran, *Phytochemistry*, 20 (1981) 2511–2519.
[12] I.M. Sims and A. Bacic, *Phytochemistry*, 38 (1995) 1397–1405.
[13] E.C. Titgemeyer, L.D. Bourquin, and G.C Fahey, *J. Sci. Food Agric.*, 58 (1992) 451–457
[14] W.S. York, A.G. Darvill, and P. Albersheim, *Plant Physiol.*, 75 (1984) 295–297.
[15] W.S. York, J.E. Oates, H. van Halbeek, A.G. Darvill, and P. Albersheim, *Carbohydr. Res.*, 173 (1988) 113–132.
[16] W.S. York, P. Albersheim, and A.G. Darvill, *Glycoconjugate J.*, 12 (1995) 446.
[17] H. Schlüpmann, A. Bacic, and S.M. Read, *Planta*, 191 (1993) 70–481.
[18] M. Dubois, K.A. Gilles, J.K. Hamilton. P.A. Rebers, and F. Smith, *Anal. Chem.*, 28 (1956) 350–356.
[19] A.G.J. Voragen, H.A. Schols, and W. Pilnik, *Food Hydrocolloids*, 1 (1986) 65–70.
[20] S.M. Read, G. Currie, and A. Bacic, *Carbohydr. Res.*, (1995), in press.
[21] P. Prehm, *Carbohydr. Res.*, 78 (1980) 372–374.
[22] I. Ciucanu and F. Kerek, *Carbohydr. Res.*, 131 (1984) 209–217.
[23] E. Lau and A. Bacic, *J. Chromatogr.*, 637 (1993) 100–103.
[24] A.L. van Geet, *Anal. Chem.*, 42 (1970) 679–680.
[25] D. Marion and K. Wüthrich, *Bichem. Biophys. Res. Comm.*, 113 (1983) 967–974.
[26] M. Rance, O.W. Sørenson, G. Bodenhausen, G. Wagner, R.R. Ernst, and K. Wüthrich, *Bichem. Biophys. Res. Comm.*, 117 (1983) 479–485.
[27] L. Braunschweiler and R.R. Ernst, *Mol. Phys.*, 53 (1983) 521–528.
[28] D.G. Davis and A. Bax, *J. Am. Chem. Soc.* 107 (1985) 2820–2821.
[29] S.P. Rucker and A.J. Shaka, *Mol. Phys.*, 68 (19839) 509–517.
[30] A.M. Gane, D. Craik, S.L.A. Munro, G.J. Howlett, A.E. Clarke, and A. Bacic, *Carbohydr. Res.* 277 (1995) 67–85.
[31] W.S. York, L.K. Harvey, R. Guillen, P. Albersheim, and A.G. Darvill, *Carbohydr. Res.*, 248 (1993) 285–301.
[32] P.K. Agrawal, *Phytochem.*, 31 (1992) 3307–3330.
[33] Y. Akiyama and K. Kato, *Phytochem.*, 21 (1982) 1325–1329.
[34] S.C. Fry, *Ann. Rev. Plant Physiol. Plant Mol. Biol.*, 46 (1995) 497–520.